CHAPTER IV

RESULTS AND DISCUSSION

4.1 Grafting of Maleic Anhydride onto Polypropylene

In this work, the effect of initiator and maleic anhydride amount and the screw speed on the grafting reaction were studied. The % grafted MA onto PP and MFI of PP-g-MA at various screw speeds, and DCP and MA concentrations are presented in Table 4.1

The grafting reaction of MA onto PP occured simultaneously with the degradation reaction of PP, but the former should be predominant in the short period of time. It be observed from Figure 4.1 that the maximum percentage of MA grafted on PP reached the maximum and was constant independent upon the screw speed of the twin screw extruder. From now on, unless otherwise stated, the screw speed was controlled constantly at 90 rpm for the preparation of the PP-g-MA used in the studies.

Upon maintaining the concentration of MA constant at 5 phr and variation of the DCP concentration, it was found that increasing of the DCP amount, i.e. the radical concentration increased, obviously resulted in the increase of the percentage of MA grafted on PP and MFI (see Figure 4.2).

When the DCP concentration of 4 phr was employed with the variation of the MA concentration, it can be observed from Figure 4.3 that the grafting level of MA onto PP decreased from 0.93 to 0.53% when the amount of MA increased from 5.0 to 7.0 phr, and afterwards it levelled off independent upon the MA concentration. In the same manner, $MFI_{2.16,\ 230^{\circ}C}$ of the resulting PP-g-MA decreased from 156 to 11.9 g/10 min with the increase of MA concentration from 5.0 to 6.5 phr and then maintained constant independent upon the MA concentration. From the current statement, it could be concluded that at 4 phr DCP the excess amount of MA more than 7.0 phr might not involve in the maleation reaction with the PP radicals.

Therefore, the most appropriate condition for the preparation of PP-g-MA, using the laboratory twin screw extruder (L/D ratio of 42/7, screw diameter of 41.8 mm) having the screw speed of 90 rpm, found in this study was that the concentrations of MA and DCP should be respectively 6.3 and 4.0 phr to obtain such the grafted copolymer having the grafting level of 0.7% and $MFI_{2.16\ kg,\ 230°C}$ of 25 g/10 min.

Table 4.1. Grafting level and $MFI_{2.16,\ 230°C}$ of PP-g-MA at various screw speeds, DCP and MA concentrations.

Screw Speed (rpm)	DCP Conc. (phr)	MA Conc. (phr)	MA Grafted onto PP (%)	$MFI_{2.16,\ 230°C}$ (g/10min)
100	1.0	5.0	0.20	5.4
90	1.0	5.0	0.20	4.4
80	1.0	5.0	0.19	4.8
60	1.0	5.0	0.21	4.9
90	1.0	5.0	0.20	9.6
90	2.0	5.0	0.40	24.5
90	3.0	5.0	0.53	50.6
90	4.0	5.0	0.93	156
90	4.0	5.0	0.93	156
90	4.0	5.5	0.86	123
90	4.0	6.0	0.74	64.0
90	4.0	6.5	0.61	11.9
90	4.0	7.0	0.53	9.7
90	4.0	8.0	0.57	10.2

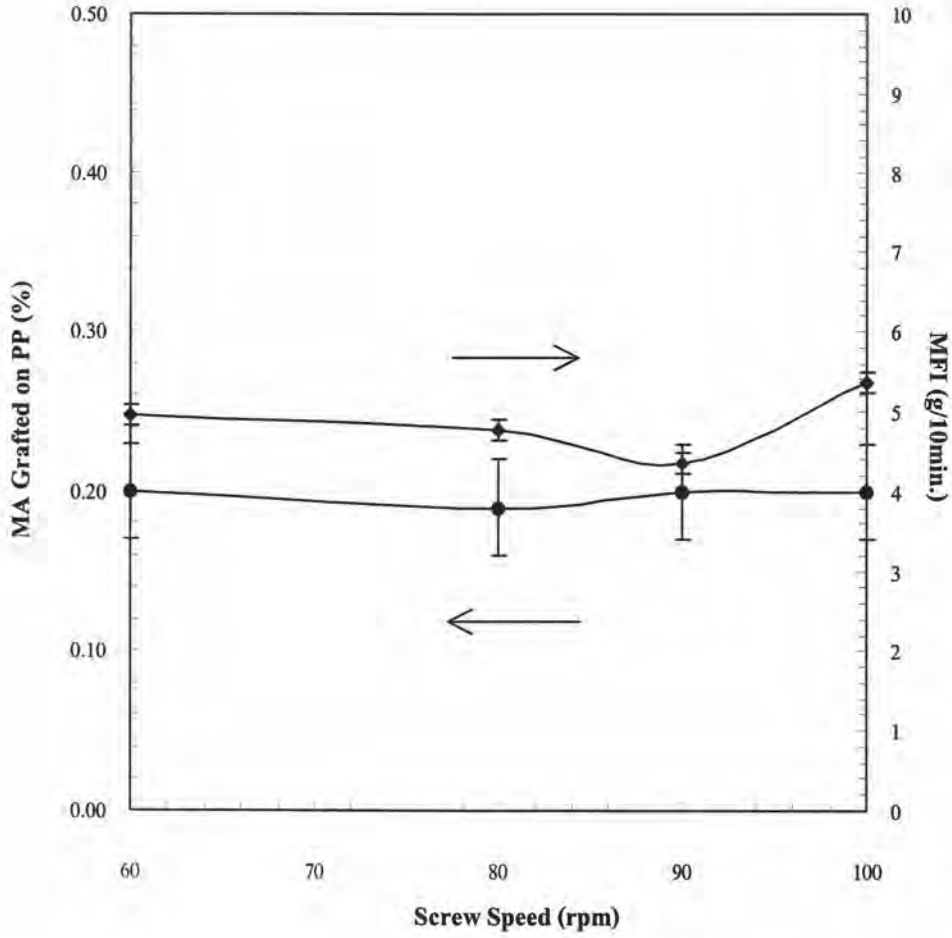

Figure 4.1 Effect of screw speed of the twin screw extruder (L/D = 42/7, and screw diameter = 41.8 mm) on the MA grafting level and $MFI_{2.16,\ 230°C}$ of PP-g-MA.

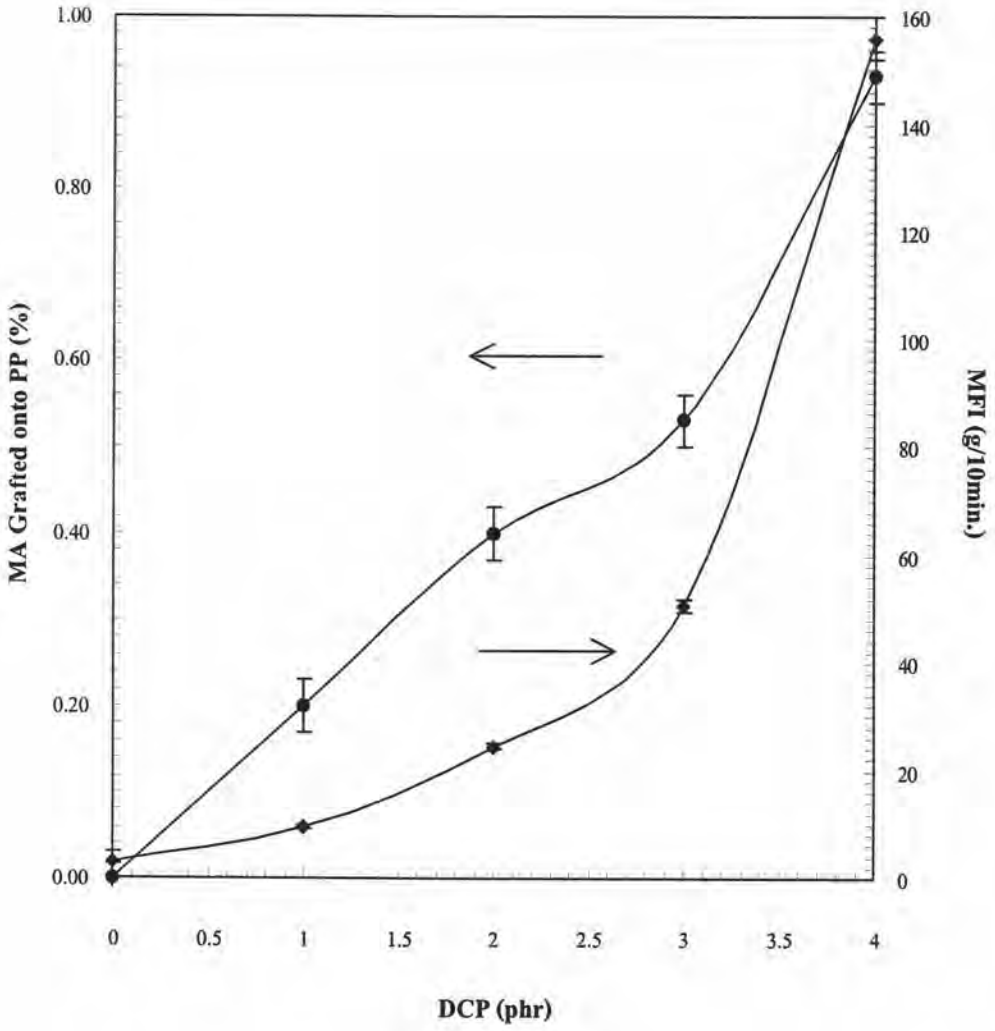

Figure 4.2 Effect of DCP concentration on the MA grafting level and $MFI_{2.16,\ 230°C}$ of PP-g-MA.

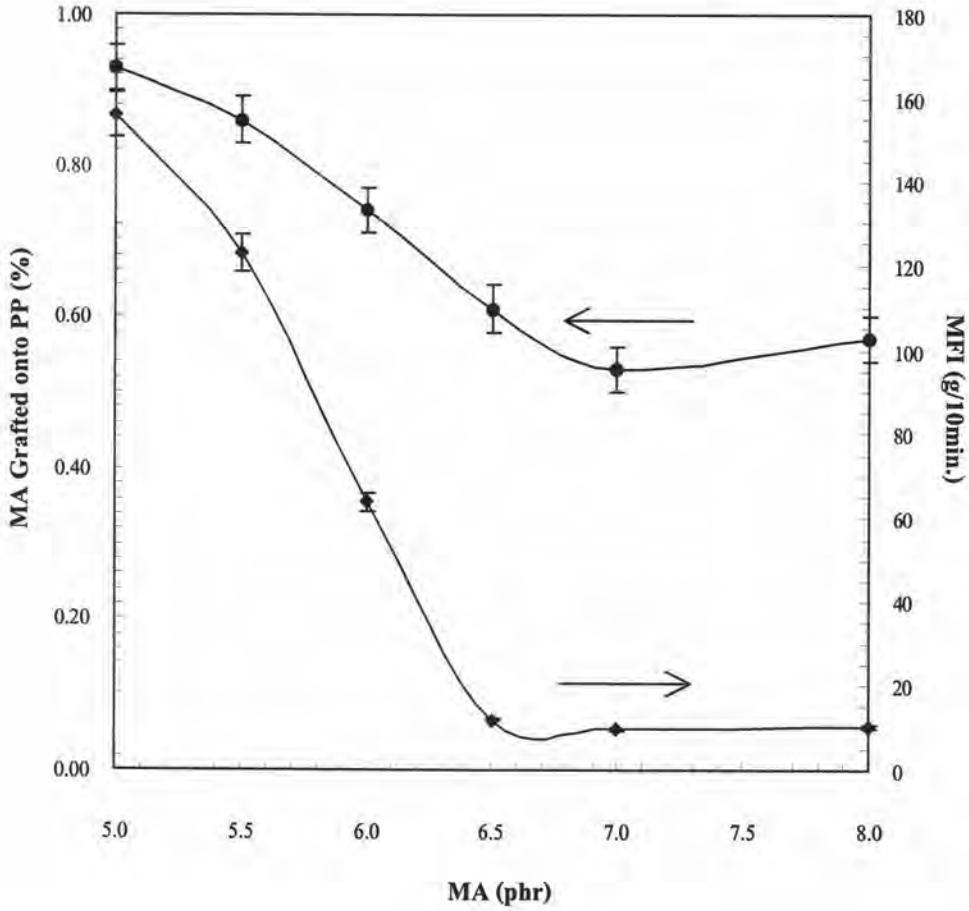

Figure 4.3 Effect of MA concentration on the MA grafting level and $MFI_{2.16,\ 230°C}$ of PP-g-MA.

4.2 Mechanical Properties of PP/EVA Blend

4.2.1 Impact Strength of PP/EVA Blend

Table 4.2 shows the impact strength, tensile strength, elongation at break and hardness of the PP/EVA blends with and without the usage of PP-g-MA compatibilizer. Figure 4.4 shows that when the EVA content in the polyblends increased from 0-40%, their impact strength minorly improved. Significant improvement was found when the EVA content in the blend composition was upto 50%. Figure 4.5 also shows the correlation of relative impact strength of PP/EVA blends to the EVA content in the blends composition ranging from 0-40%. The relative impact strength is defined as

$$\text{Relative impact strength} = \frac{\text{Impact strength of PP blend}}{\text{Impact strength of PP}} \quad (4.1),$$

when the impact strength of PP was 18.7 J/m.

The values of relative impact strength for 9, 12 and 19% VA contents in EVA were obtained from the work of Gupta et al [9]. It was apparently that the EVA having higher VA content blended with PP showed to be better impact modifier than that having lower content (see Figure 4.5). It was also observed from Figure 4.5 that the jump of the impact strength of the PP/EVA blends when using different VA content of the EVA was found in the same manner as that just mentioned. For example, when the VA content was of 19%, the impact strength jumped when the EVA content in the polyblend increased from 10 to 15%. In this study it was found two steps of rapidly changes of impact strength. Firstly, when the EVA content was more than 10 %. The linear relationship of the impact strength of the polyblends having the EVA contents of 10-40% w/w was observed. The second rapidly changes of this property was found when the EVA content increased from 40 to 50% as shown in Figure 4.4.

PP-g-MA in the ranges of 0-10 phr was employed as the compatibilizer in preparation of PP/EVA blend. Figure 4.6 shows the relationship of impact strength to the EVA content in the blend composition. Similar tends to Figure 4.4 was found. At the constant EVA content in the blend composition, their impact strength when using 2 phr PP-g-MA as the compatibilizer slightly increased. At the other concentrations of PP-g-MA, there might be the effect of the abundance of strongly interaction of anhydride group presented in the grafted copolymer so that it did not act as the good compatibilizer. The differences of impact strength at different blending ratios of EVA to PP were accompanied by the differences in the morphology of EVA dispersion phase. Figures 4.11-4.16 show photographs of the PP/EVA blend specimens as obtained from SEM microscope.

Table 4.2 Mechanical properties of PP/EVA blends with various compatibilizer concentrations.

PP/EVA	PP-g-MA (phr)	Mechanical Properties			
		Impact Strength (J/m)	Tensile Strength (MPa)	Elongation@ Break (%)	Hardness (R Scale)
100/0	0	18.7	37.91	20.1	112.3
95/5	0	38.2	36.23	17.8	111
	2	38.7	36.88	21.2	112
	4	27.7	36.46	22.6	112
	6	32.7	36.46	21.9	110
	10	25.4	35.23	20.7	111
90/10	0	39.5	30.99	210	108
	2	52.3	31.71	162	109
	4	46.3	31.80	152	108
	6	43.8	32.57	181	108
	10	41.0	32.98	196	109
80/20	0	74.0	27.25	461	99.8
	2	86.6	28.00	330	100
	4	74.7	28.52	255	101
	6	71.8	28.27	302	100
	10	80.1	28.29	320	100
70/30	0	110	23.75	598	88.7
	2	114	25.00	599	89.7
	4	109	25.23	580	89.3
	6	111	25.20	617	90.2
	10	110	25.35	590	91.3
60/40	0	154	21.67	627	76.6
	2	165	21.04	637	76.6
	4	137	21.27	606	76.6
	6	131	22.03	184	79.2
	10	126	23.43	170	80.1
50/50	0	540	17.14	472	69.9
	2	553	17.26	428	71.6
	4	494	18.23	285	71.2
	6	493	19.20	234	71.5
	10	355	20.05	285	70.8

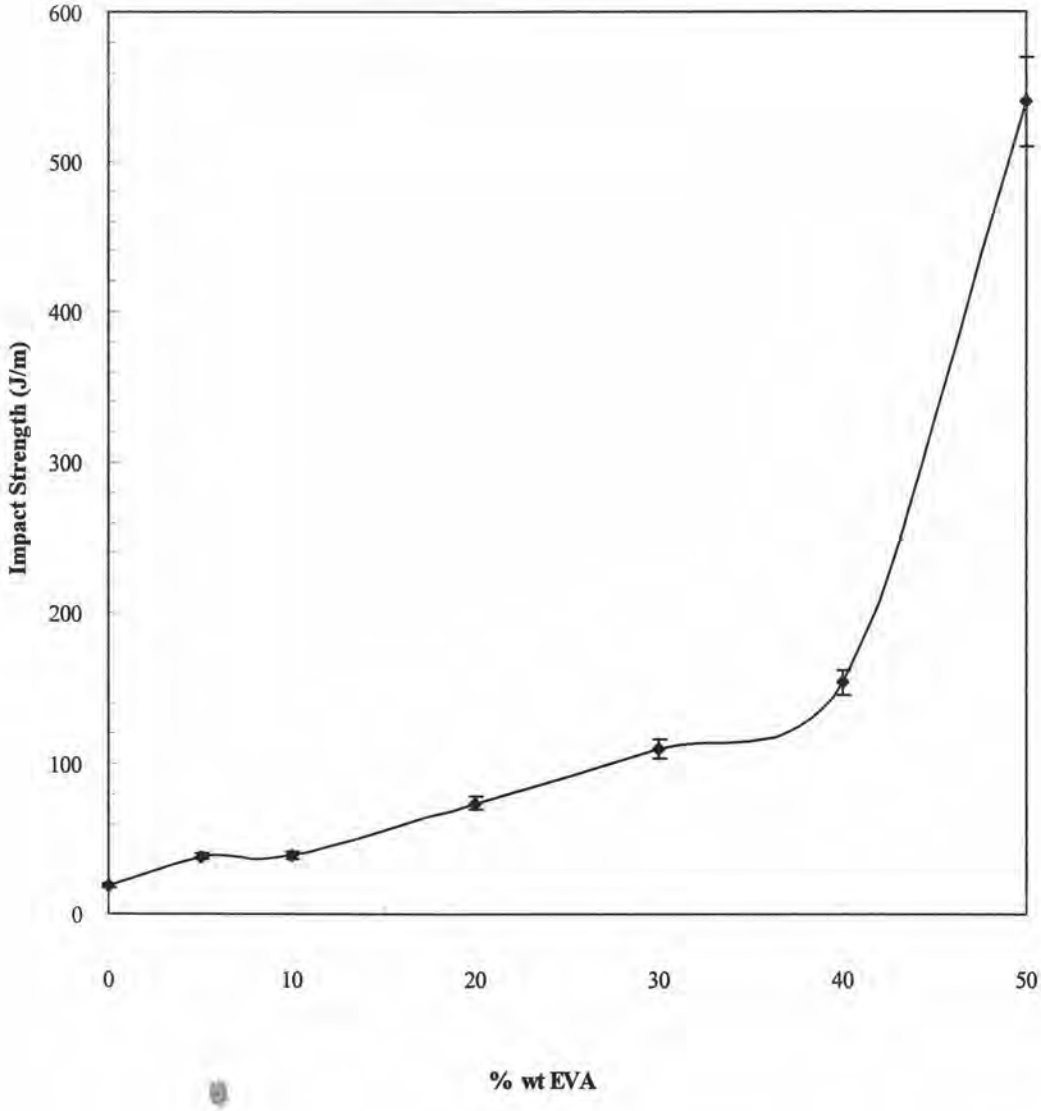

Figure 4.4 Impact strength of PP/EVA blends against % by weight of EVA in the blend composition.

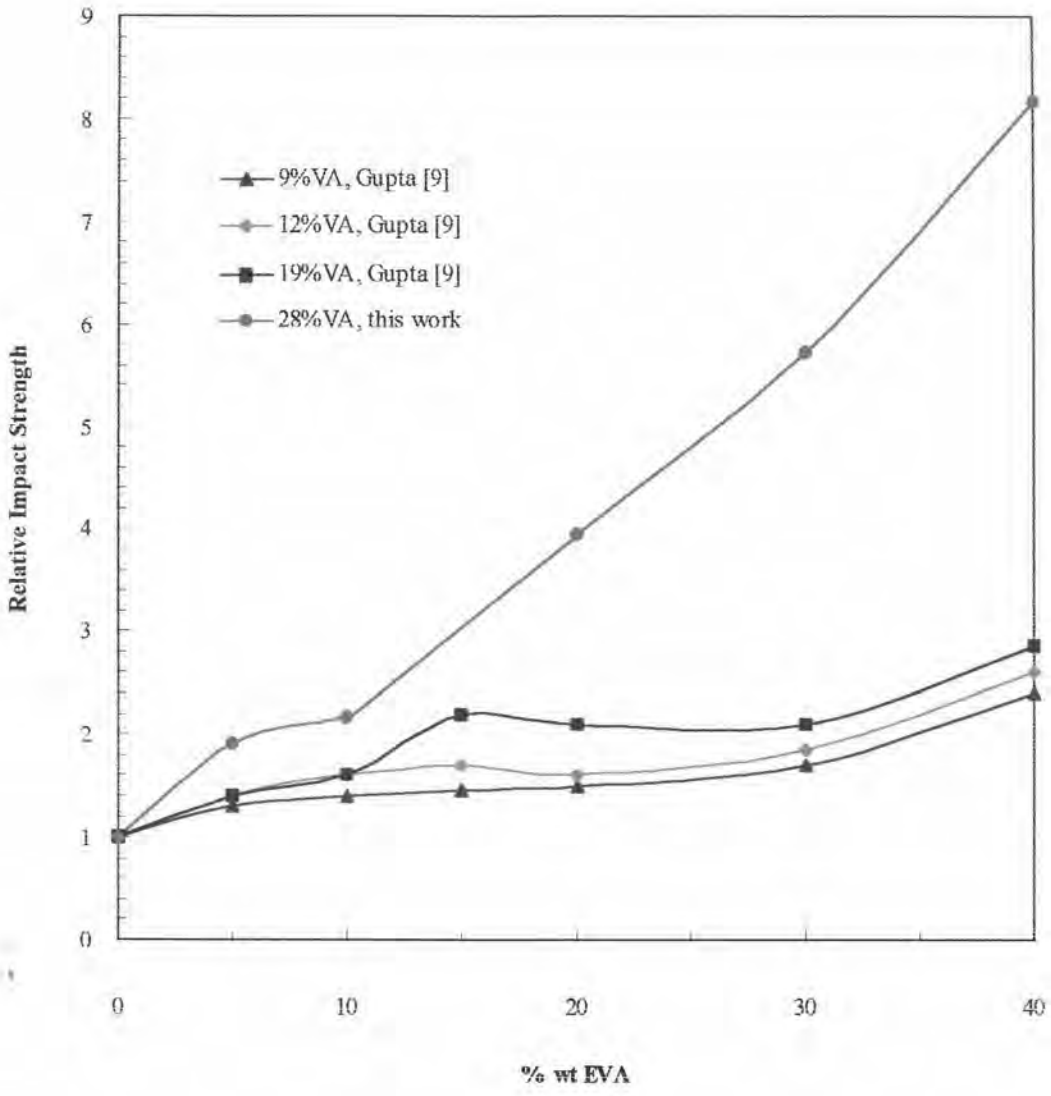

Figure 4.5 Impact strength of PP/EVA blends with various %VA contents in EVA.

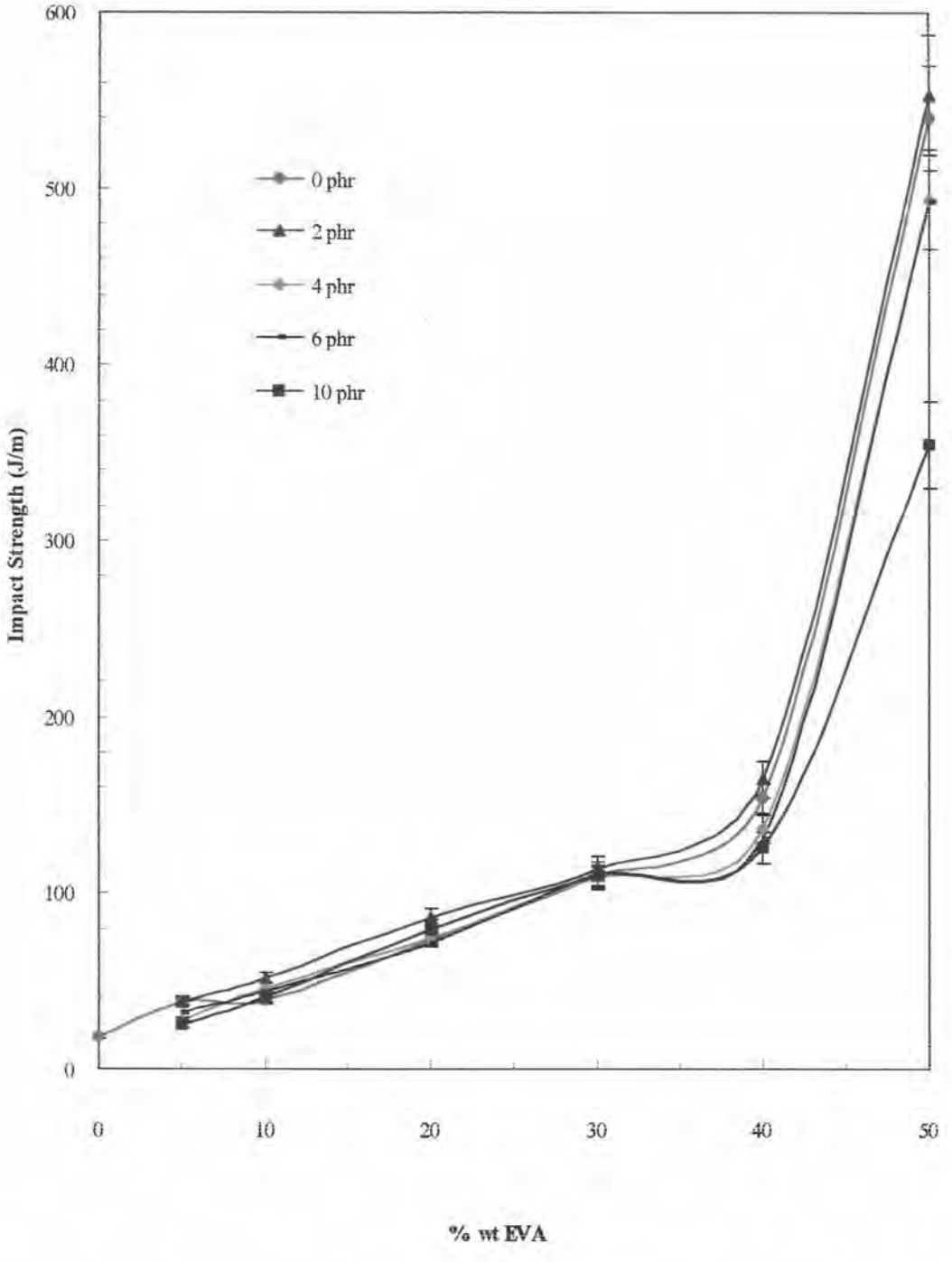

Figure 4.6 Impact strength of PP/EVA blends against % by weight of EVA in the blend composition at various amounts of PP-g-MA.

The relative impact strength of each polyblend system to that of PP are given in Table 4.3. Plot of the relative impact strength against EVA content is shown in Figure 4.7. EVA with and without 2 phr PP-g-MA seemed to be a good candidate for the impact strength improvement of PP and even superior than other elastomers but inferior to the PP/SEBS blend when the SEBS level was upto 20%. However, the PP/EVA blend prepared in this study showed better impact strength improvement than SEBS at the other contents in the blend composition.

Table 4.3 Relative impact strength of the blends of PP with various elastomers.

Blending Ratio PP/Elastomer	Relative Impact Strength						
	EVA[b]	EVA+2 phr PP-g-MA[b]	EVA-12[a,c]	EPR[a]	PBu[a]	SEBS[a]	EPDM[a]
100/0	1	1	1	1	1	1	1
95/5	1.91	2.04	1.4	-	1.4	1.5	-
90/10	2.18	2.86	1.6	-	1.45	2.3	1.35
85/15	-	-	1.7	1.9	1.45	3.0	2.0
80/20	3.95	4.63	1.6	-	-	5.5	2.1
75/25	-	-	-	-	1.5	-	-
70/30	5.72	6.13	1.85	-	1.5	-	4.5
60/40	8.17	8.58	2.6	-	-	-	-

a : from Gupta [9]

b : from this study

c : EVA with 12% VA content [9]

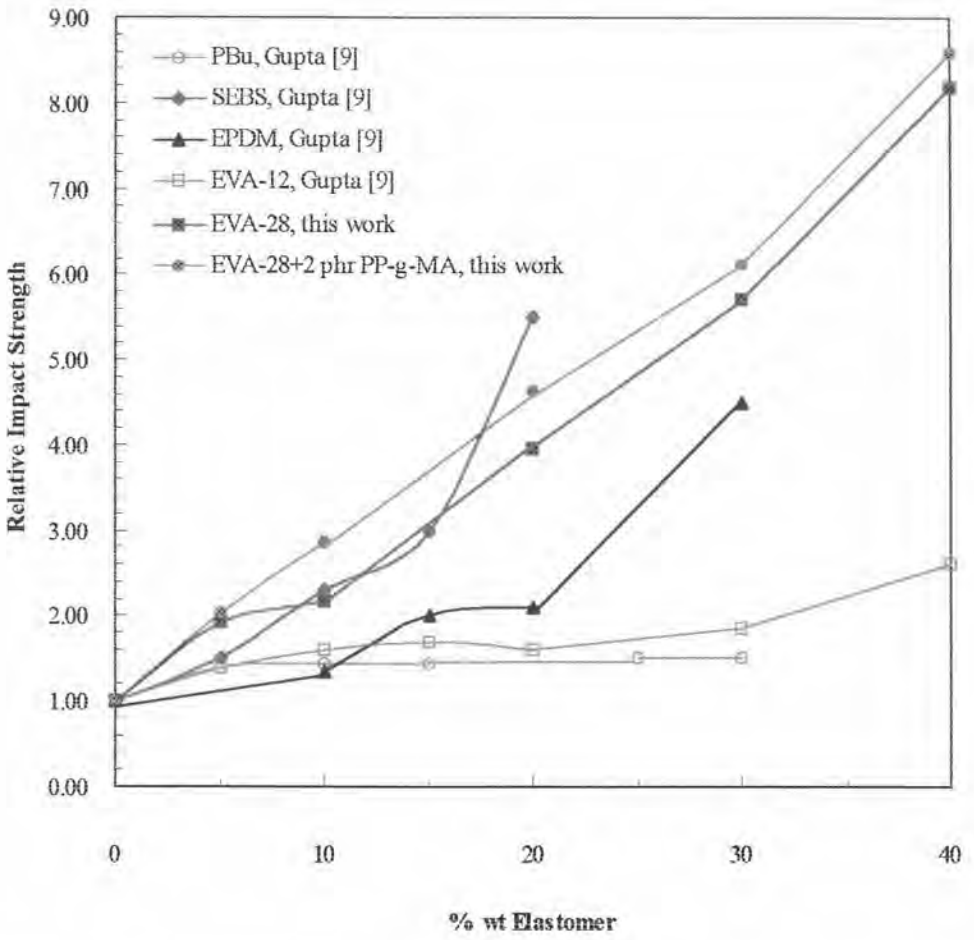

Figure 4.7 Plot of relative impact strength of the blends of PP with various types of elastomers against the amount of elastomer in the blend.

4.2.2 Tensile Strength of PP/EVA Blend

Effect of EVA with and without PP-g-MA compatibilizer on the tensile strength of polyblend is shown in Figure 4.8. The curves were similar to one another at all PP-g-MA concentration studied, particulary shown the decrease of tensile strength with the increase of EVA content in the blends. Thus it could be conclude that the increase of EVA content in the blend composition on PP provided poorer the tensile strength and PP-g-MA had not affect on the this property.

4.2.3 Elongation at Break of PP/EVA Blend

Effect of EVA with and without PP-g-MA on the elongation at break of the polyblend is shown in Figure 4.9. A constant elongation at break was found when the polyblend having 5% EVA in the blend composition, followed by a rapid increase upto 30% EVA, and then a slow rise upto 40% EVA content, finally a rapid decrease of elongation at break with the increase of EVA content in the polyblend. The usage of PP-g-MA in PP/EVA blend slightly decreased the elongation at break when the EVA content in the blend composition was about 0-30% and highly decreased when the EVA content in the polyblend was upto 40-50%, especially with the high concentration of PP-g-MA used. The decrease of elongation at break with the usage of high concentration of PP-g-MA in the polyblend might be due to the interaction of anhydride group.

4.2.4 Hardness of PP/EVA blend

Effect of EVA with and without the usage of PP-g-MA compatibilizer on hardness of PP/EVA blends is shown in Figure 4.10. The initial slow down of this property was upto 10% EVA in the polyblend, and then a rapidly decrease with the increase of EVA content in the blend compositions. The hardness of the polyblend at the constant blending ratio was similar for all of the PP-g-MA concentration used.

This could be concluded that PP-g-MA did not affect on the hardness improvement of PP/EVA blends.

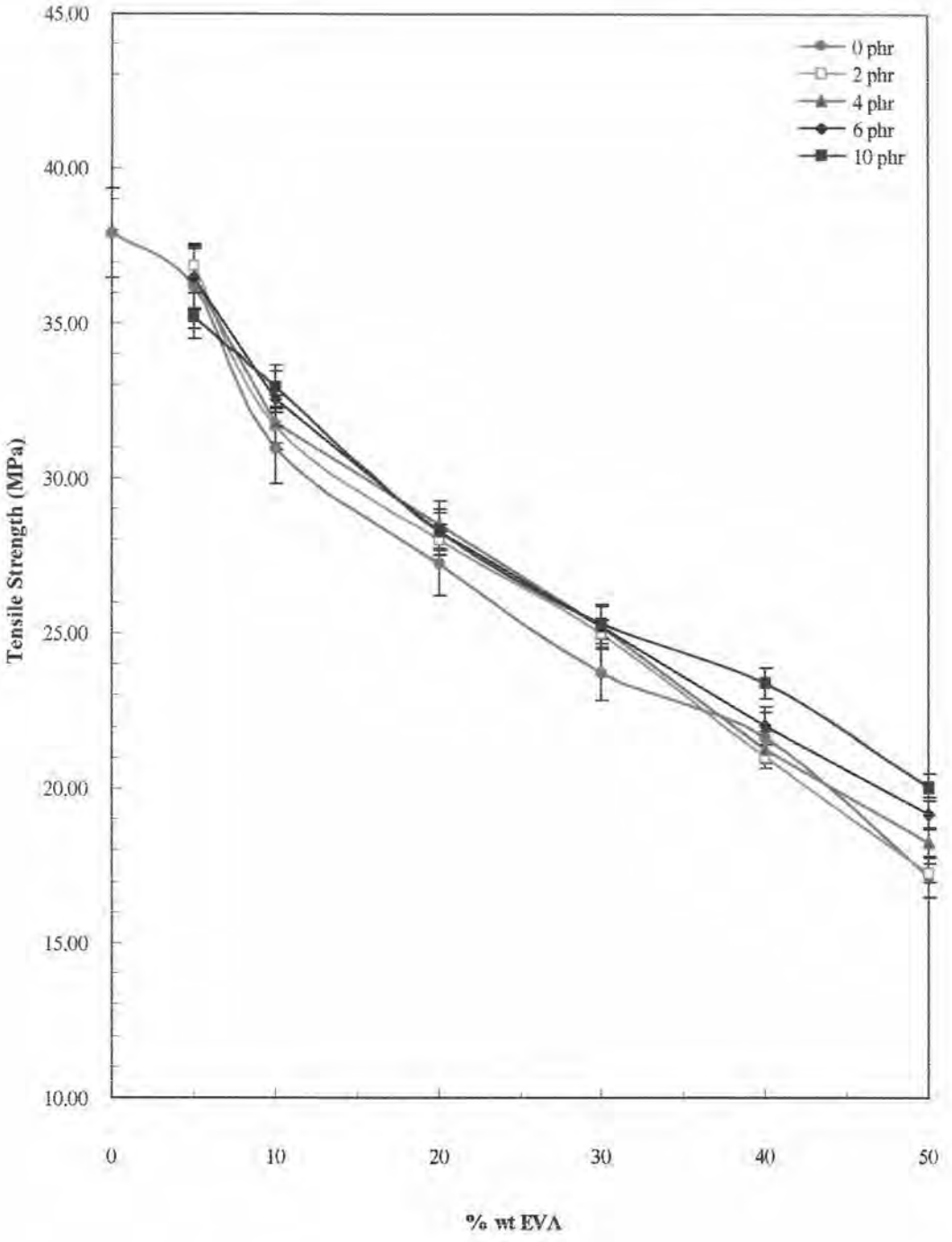

Figure 4.8 Tensile strength as a function of EVA content of PP/EVA blends with various amounts of PP-g-MA compatibilizer.

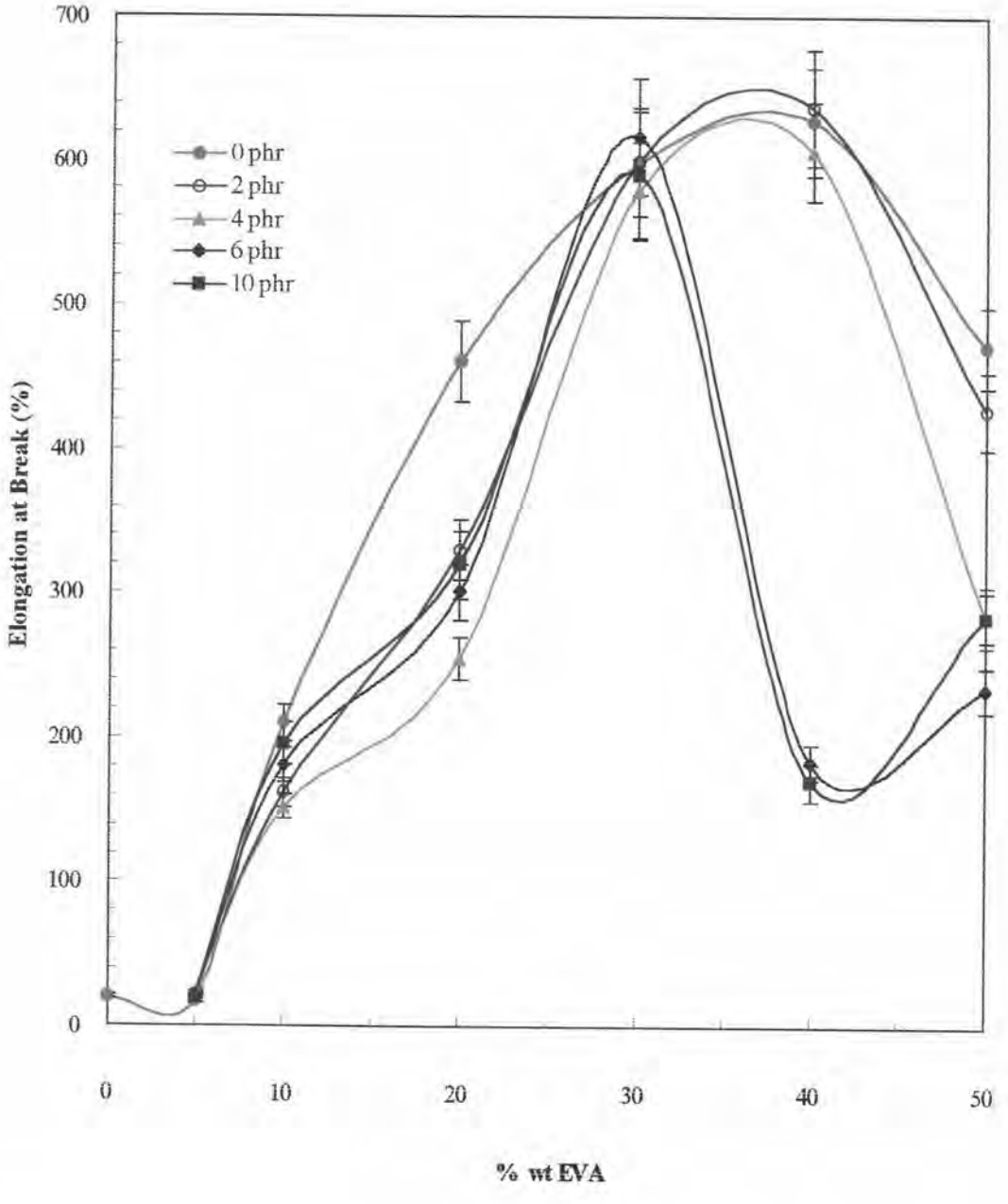

Figure 4.9 Elongation at break as a function of EVA content of PP/EVA blends with various amounts of PP-g-MA compatibilizer.

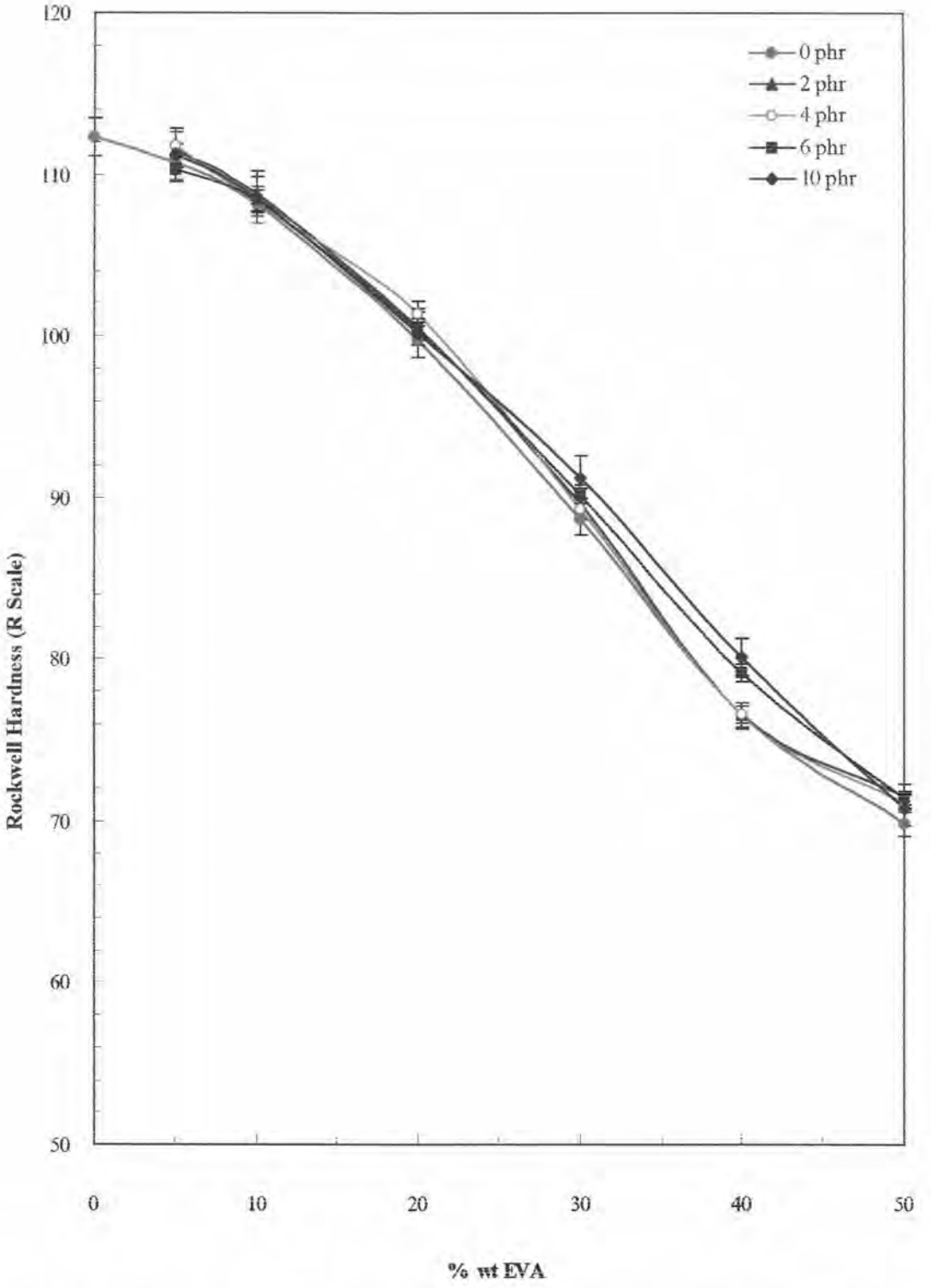

Figure 4.10 Rockwell Hardness as a function of EVA composition of PP/EVA blends with various amounts of PP-g-MA compatibilizer.

4.3 Morphology of PP/EVA Blend

The scanning electron microscope was employed to investigate the morphology and compatibilization of PP/EVA blends. Figure 4.11-4.16 show the surface of PP/EVA blend at various contents of EVA and compatibilizer.

Two-phase morphology is clearly observed in all compositions of the polyblends (see Figure 4.11). The average sizes of dispersed EVA droplets in the PP matrix increased from 0.3 to 0.6 μm as well as their quantities with the increase of EVA content in the blend composition from 5-30%. The EVA droplets were not bigger than 0.6 μm even the EVA content in the blend composition was upto 30-50%. At 50% EVA of the polyblend, it was observed that there were a large number of elongated EVA that might be formed by coalescence of several EVA droplets. The rapid increased impact strength when the EVA content in the blends was 50% might be due to the EVA rubber phase formed the continuous phase with small EVA droplets interface between that phase with PP matrix.

The changes of droplet sizes of the dispersed EVA in the polyblends that contained PP-g-MA compatibilizer are shown in Figures 4.12 to 4.16. The variation of average size of EVA droplets with the EVA composition in the polyblend with and without the compatibilizer are given in Table 4.4. It was observed that there was not clear morphological improvement from that without the usage of the compatibilizer. Therefore, it is concluded that PP-g-MA was slightly affected on the compatibility of PP/EVA blends. Either it was not necessarily required for the improvement of impact strength of the polyblend.

Table 4.4 Ranges of droplet sizes of dispersed EVA in the polyblend.

PP/EVA	PP-g-MA (phr)	Range of Droplet Size (μm)	Average Droplet Size (μm)
90/10	0	0.3-0.4	0.3
	2	0.1-.04	0.2
	6	0.1-0.4	0.3
80/20	0	0.2-0.7	0.4
	2	0.1-0.5	0.3
	6	0.3-0.7	0.5
70/30	0	0.2-1.0	0.6
	2	0.4-1.0	0.7
	6	0.3-1.0	0.5
60/40	0	0.1-1.5	0.6
	2	0.3-1.3	0.5
	4	0.2-0.9	0.5
	6	0.3-1.0	0.6
	10	0.1-1.2	0.6
50/50	0	0.1-0.7	0.4
	2	0.1-1.2	0.6
	4	0.1-1.2	0.5
	6	0.1-0.9	0.5
	10	0.1-2.1	0.7

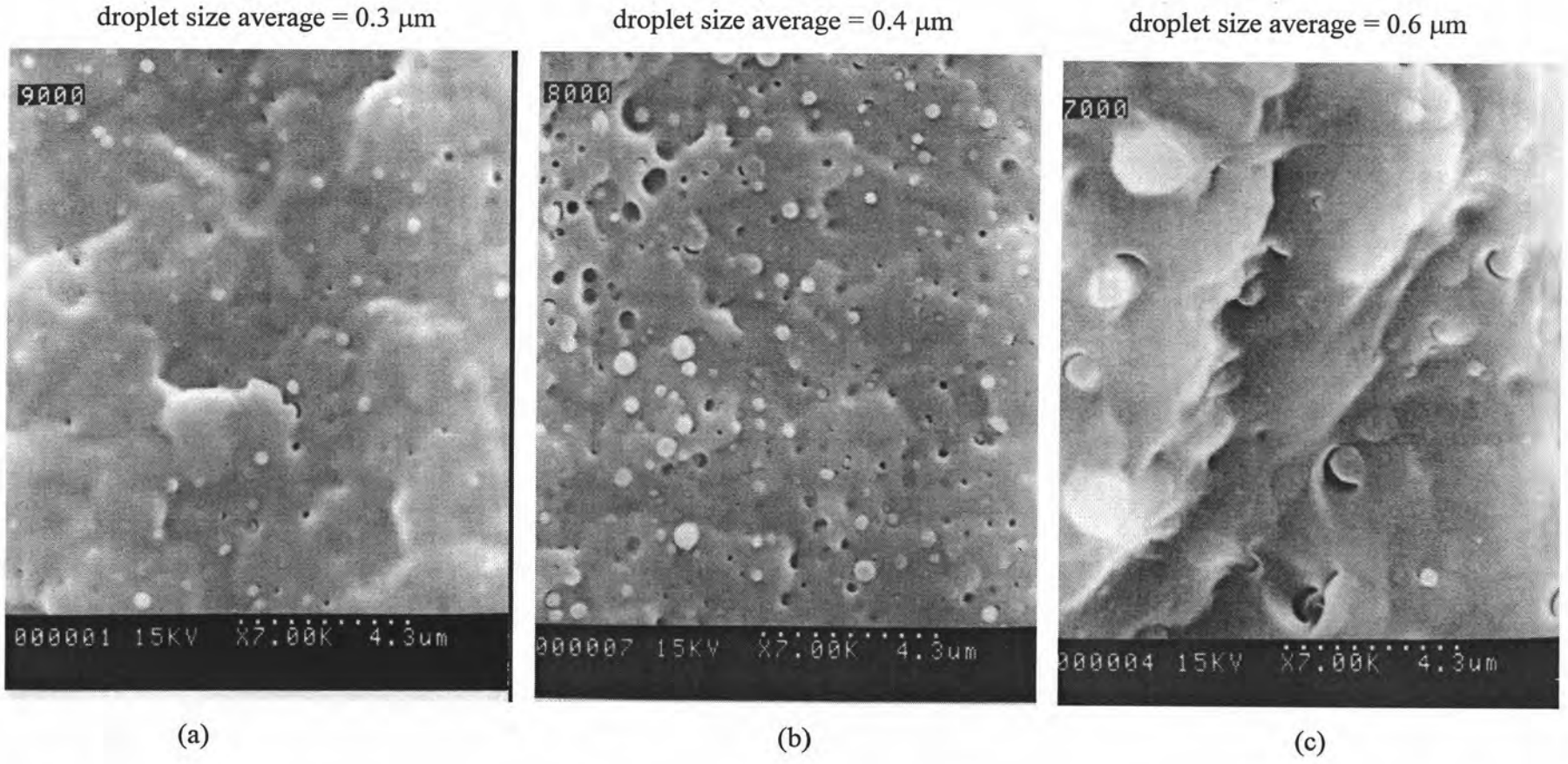

Figure 4.11 Scanning electron micrographs (magnification 7,000 times) of PP/EVA blends with variation of EVA content (% wt) (0 phr PP-g-MA): (a) 10; (b) 20; (c) 30; (d) 40; (e) 50.

droplet size average = 0.6 μm

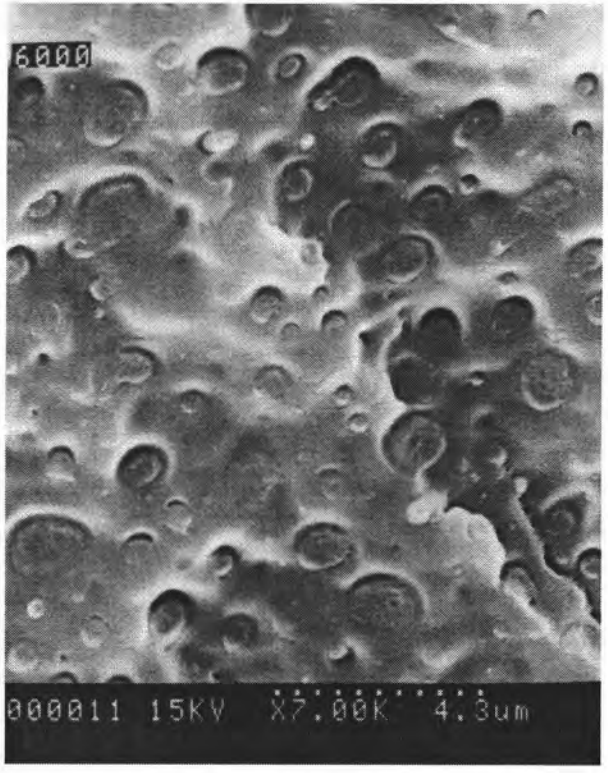

(d)

droplet size average = 0.4 μm

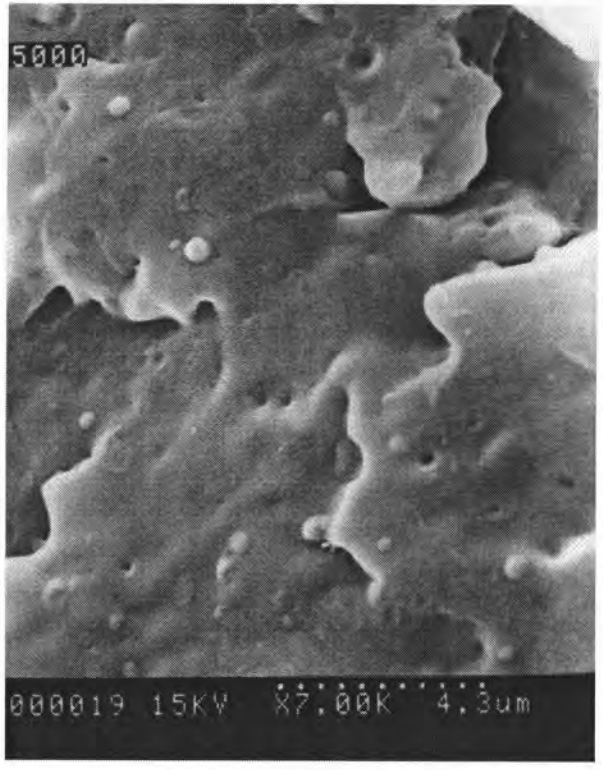

(e)

Figure 4.11 (Continue)

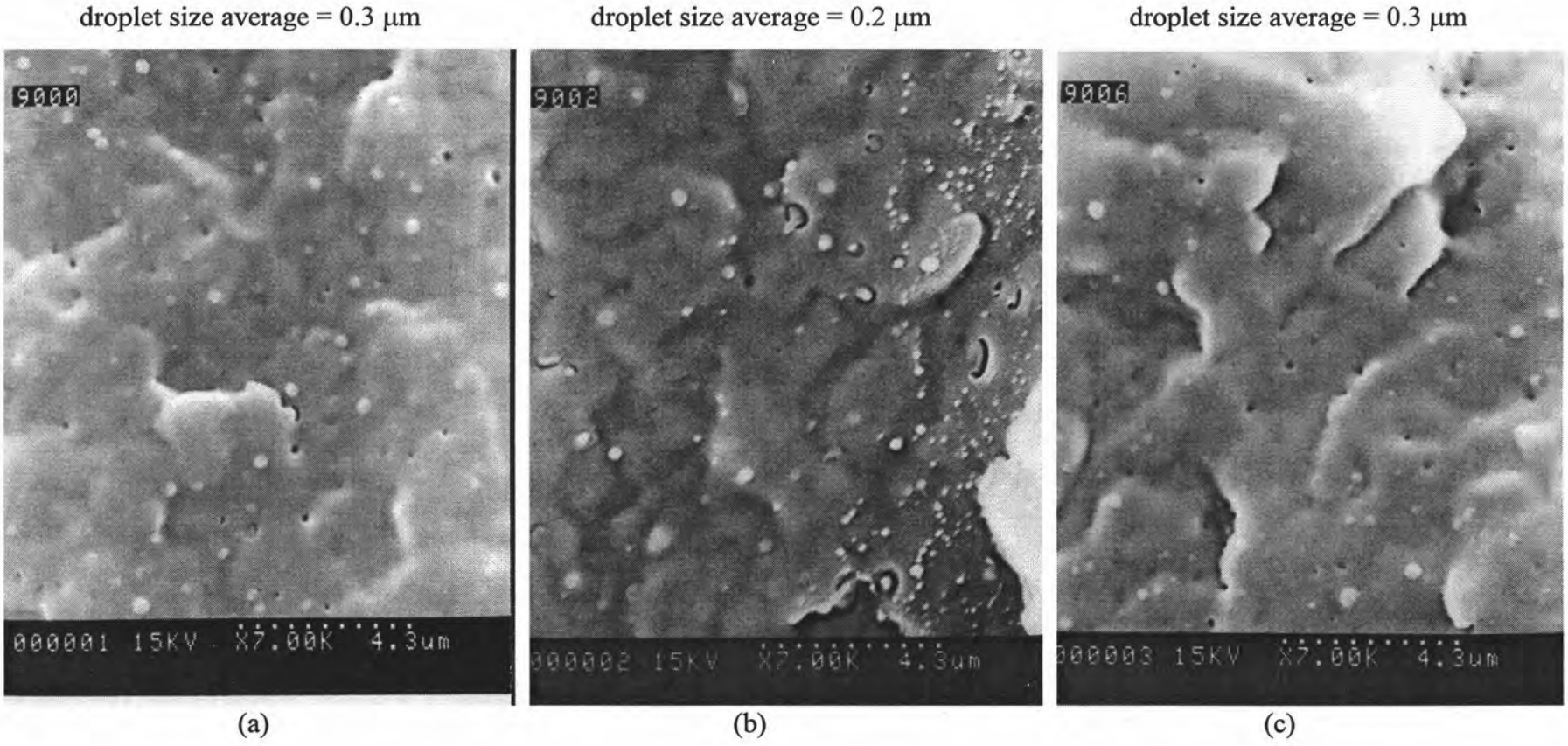

Figure 4.12 Scanning electron micrographs (magnification 7,000 times) of PP/EVA blends with 10% by weight EVA. PP-g-MA was used as the compatibilizer: (a) 0 phr; (b) 2 phr; (c) 6 phr.

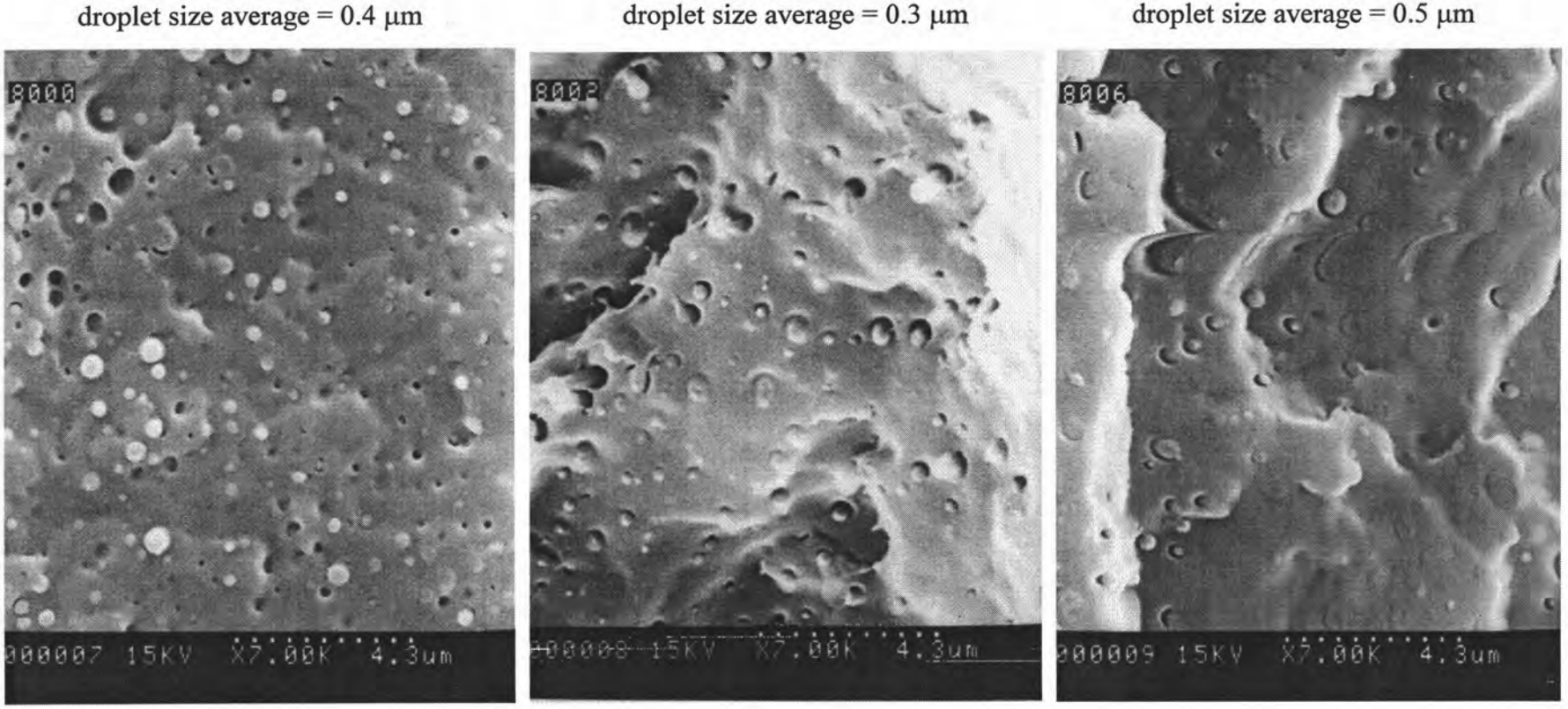

Figure 4.13 Scanning electron micrographs (magnification 7,000 times) of PP/EVA blends with 20% by weight EVA. PP-g-MA was used as the compatibilizer: (a) 0 phr; (b) 2 phr; (c) 6 phr.

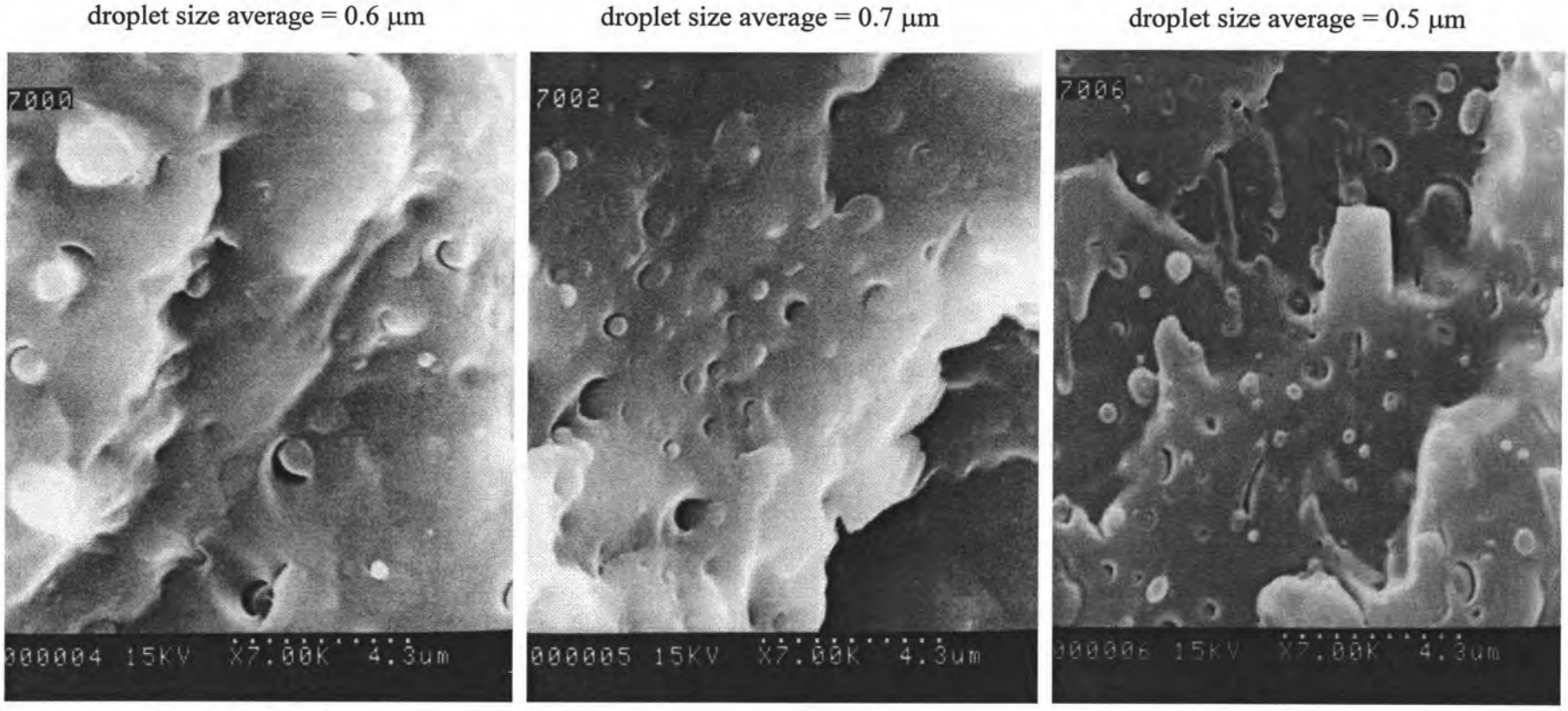

Figure 4.14 Scanning electron micrographs (magnification 7,000 times) of PP/EVA blends with 30% by wt EVA. PP-g-MA was used as the compatibilizer: (a) 0 phr; (b) 2 phr; (C) 6 phr.

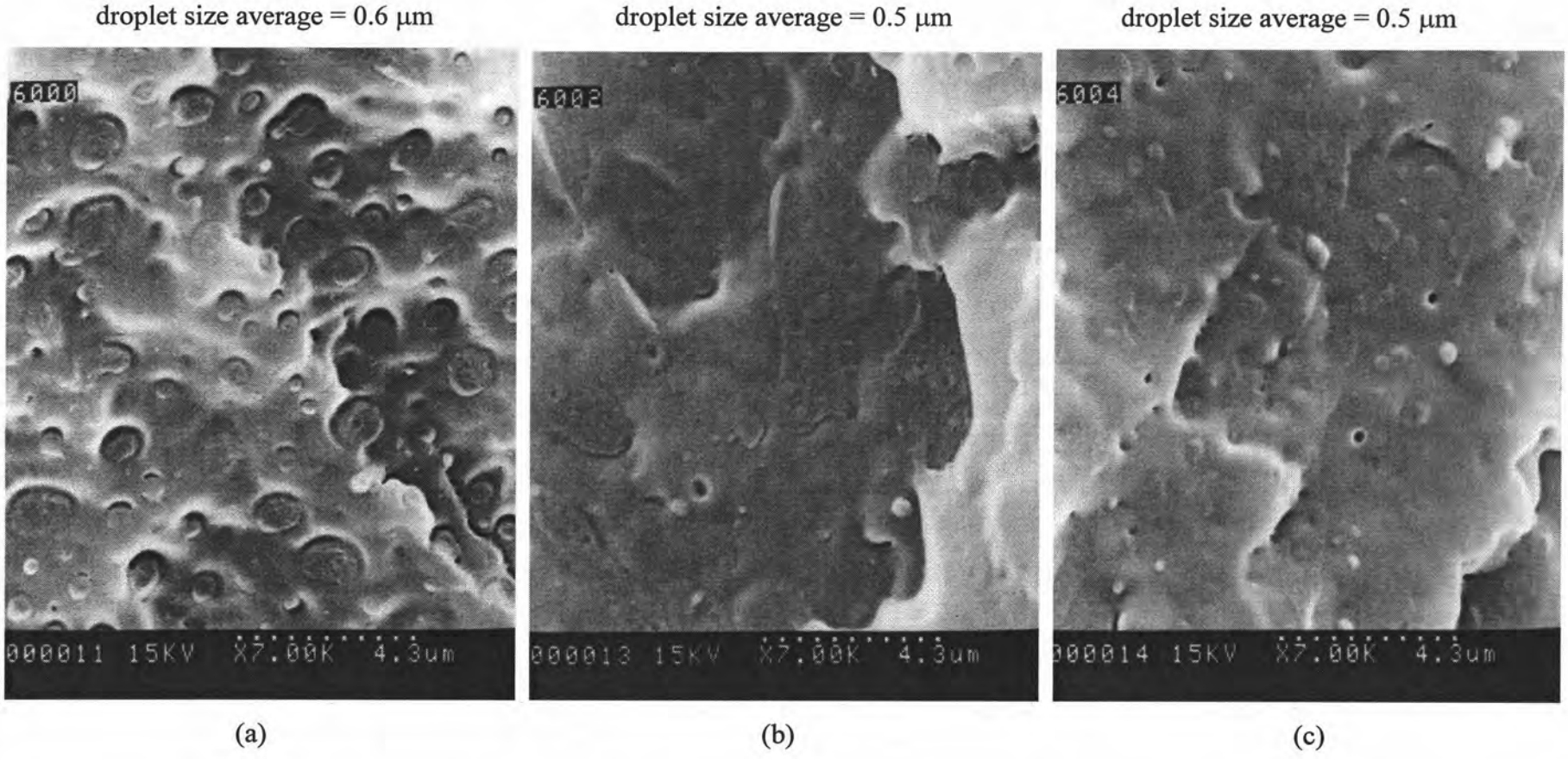

Figure 4.15 Scanning electron micrographs (magnification 7,000 times) of PP/EVA blends with 40% by wt EVA. PP-g-MA was used as the compatibilizer: (a) 0 phr; (b) 2 phr; (c) 4 phr ; (d) 6 phr; (e) 10 phr.

droplet size average = 0.6 μm

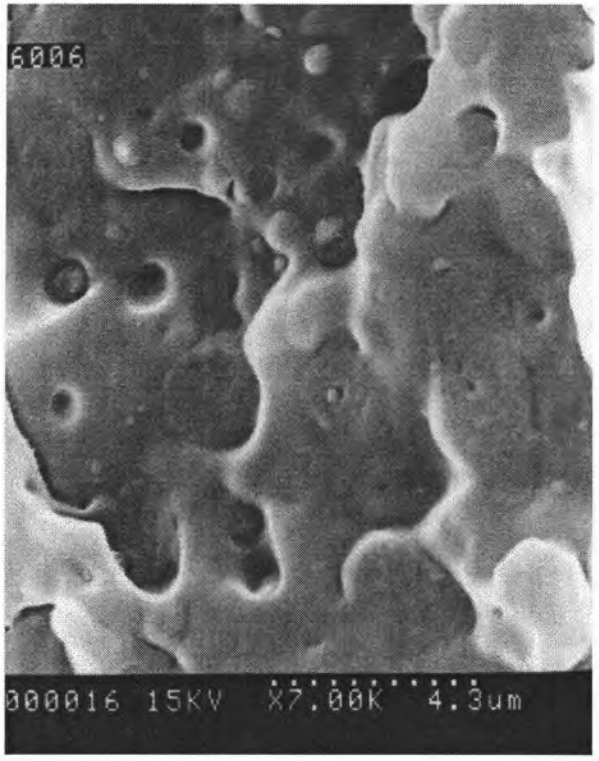

(d)

droplet size average = 0.6 μm

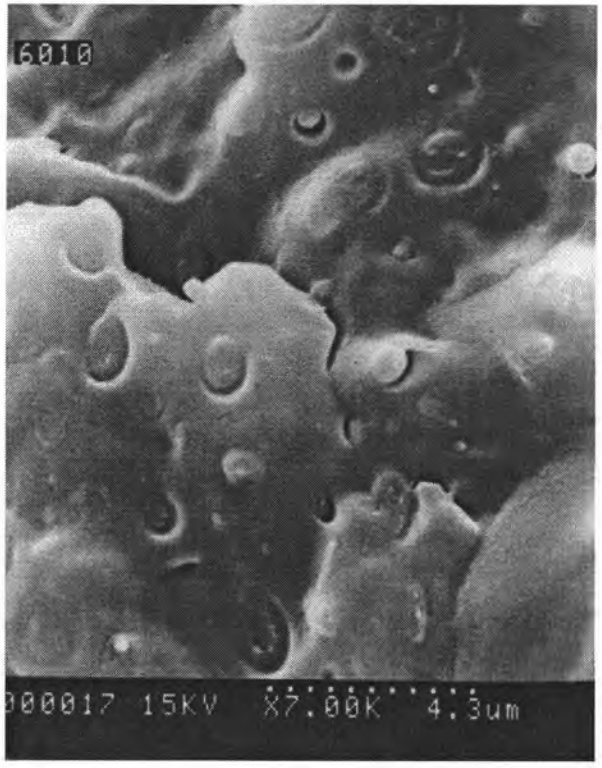

(e)

Figure 4.15 (Continue)

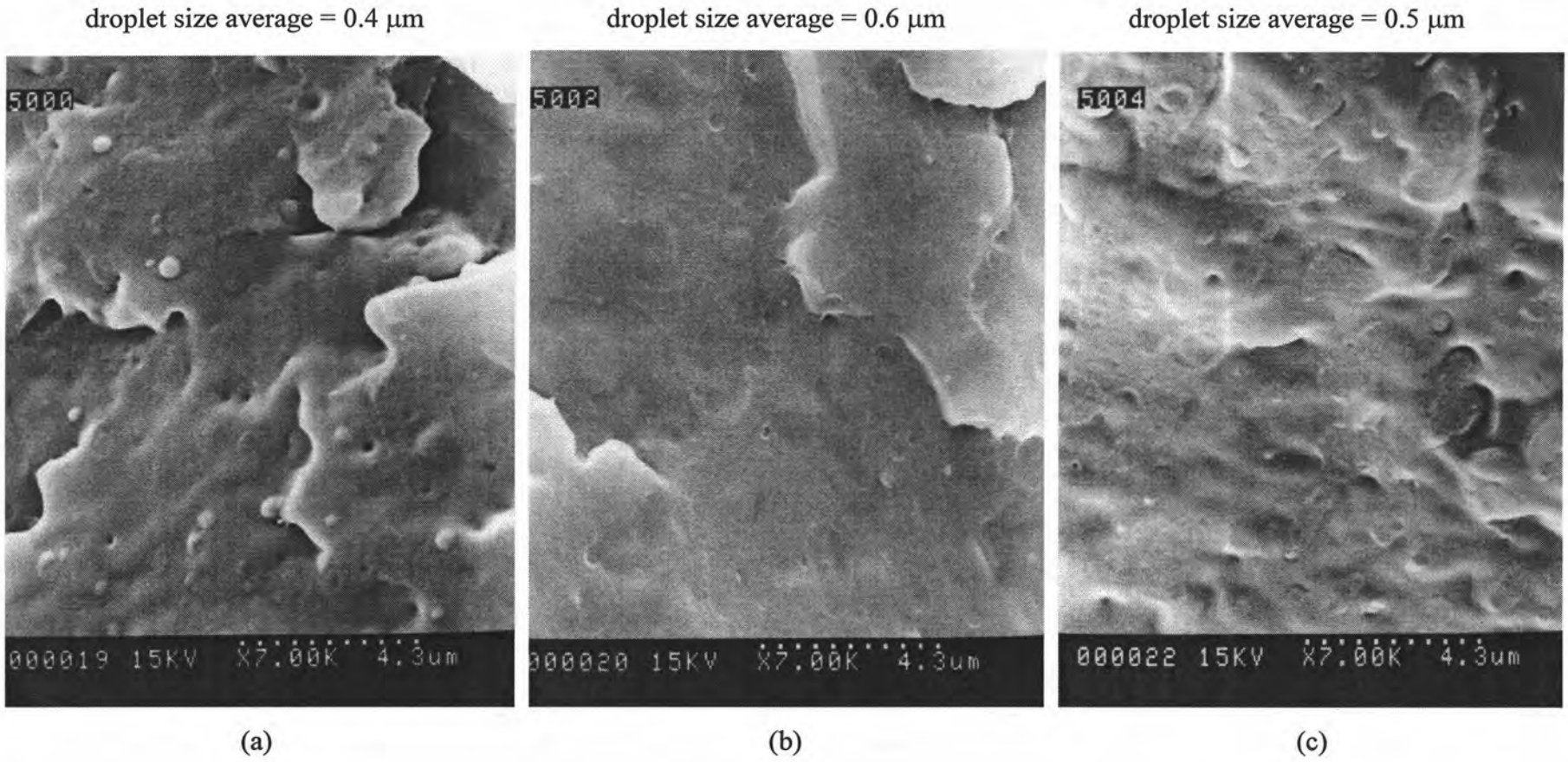

Figure 4.16 Scanning electron micrographs (magnification 7,000 times) of PP/EVA blends with 50% by weight EVA. PP-g-MA was used as the compatibilizer: (a) 0 phr; (b) 2 phr; (c) 4 phr; (d) 6 phr; (e) 10 phr.

droplet size average = 0.5 μm

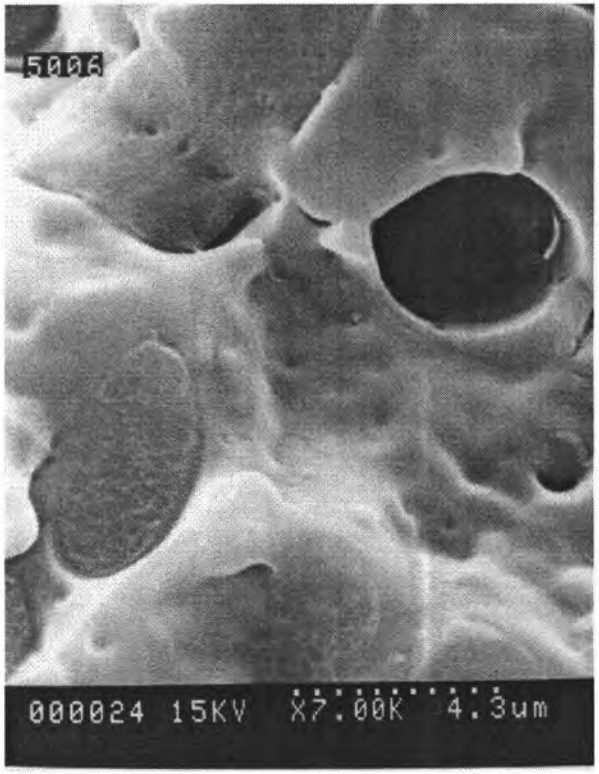

(d)

droplet size average = 0.7 μm

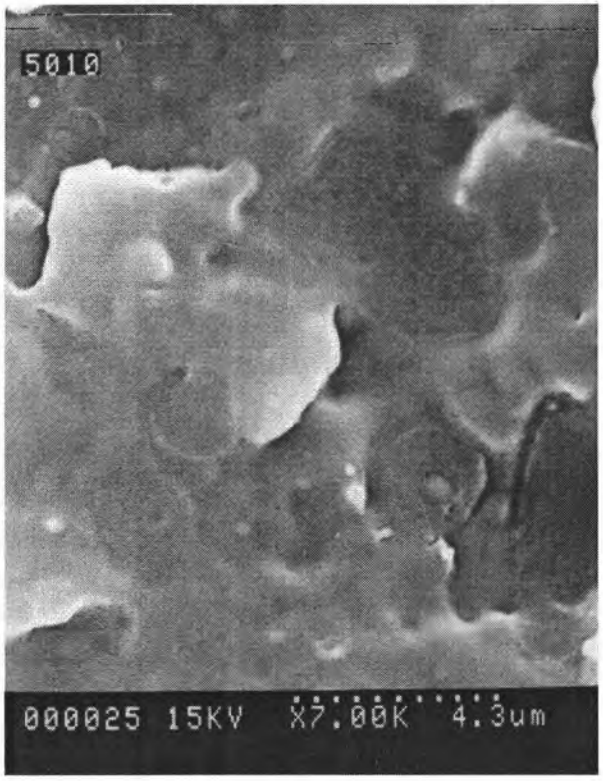

(e)

Figure 4.16 (Continue)

4.4 Miscibility Study of PP/EVA Blends by DSC Measurement

Effect of EVA and PP-g-MA on glass transition temperature of PP/EVA blend was investigated. The value of T_g and T_m of different PP/EVA blends are presented in Table 4.5.

Figure 4.17 shows the plot of T_g of PP/EVA blend with and without PP-g-MA compatibilizer. In the case of without compatibilizer, points in the figure were the average values of T_g at specific amount of EVA in the blend composition. It is apparently that T_g's of PP/EVA blends at 0-30% EVA in the blend composition without the compatibilizer were not much different from the theoretically values calculated from Equation (2.5). From the DSC thermograms in Figure 4.18, separated two glass transitions were observed when the EVA composition in the blend was more than 30%. T_m's of PP/EVA blend at all blending compositions were not different from that of the original PP (see Figure 4.19), that EVA could be only miscible with the amorphous region of PP in the ranges of 0-30% EVA in the blend composition.

PP-g-MA improved the miscibility of EVA in amorphous region of PP when its composition in the blend was 40%. Only 2-4 phr preferably 2 phr PP-g-MA improved significantly of the miscibility, and the other concentrations did not. For the 50% EVA in the blend composition, 6 phr of PP-g-MA improved the miscibility. It was observed from the DSC thermogram that at higher concentration more than 4 phr of PP-g-MA and 40-50% EVA content in the blend composition, two separate T_g's were also observed (see Figures 4.20-4.21). It implied that PP-g-MA decreased miscibility of the PP/EVA blend at high dosage of the compatibilizer.

Table 4.5 T_g and T_m of PP/EVA blends with various PP-g-MA concentrations.

EVA (%)	PP-g-MA (phr)	DSC Results	
		T_g (°C)	T_m (°C)
PP	-	7.36	158.89
EVA	-	-39.27	59.93
5	0	5.60	159.33
	2	-6.24	157.58
	4	-1.90	157.82
	6	-20.47	158.23
	10	-27.01	158.98
10	0	3.94	156.78
	2	-11.92	158.02
	4	-1.27	157.57
	6	-26.80	158.33
	10	-24.12	157.27
20	0	1.49	157.49
	2	-22.30	158.60
	4	-8.04	157.18
	6	-12.13	159.71
	10	-6.37	159.68
30	0	-3.98	157.68
	2	-29.56	158.78
	4	-28.70	158.44
	6	-17.10	159.12
	10	-19.62	159.16
40	0	-21.80	157.60
	2	-12.49	157.28
	4	-18.42	158.56
	6	-30.96	158.54
	10	-28.07	158.31
50	0	-30.09	157.82
	2	-23.24	158.73
	4	-20.80	159.02
	6	-13.28	159.07
	10	-32.323	158.34

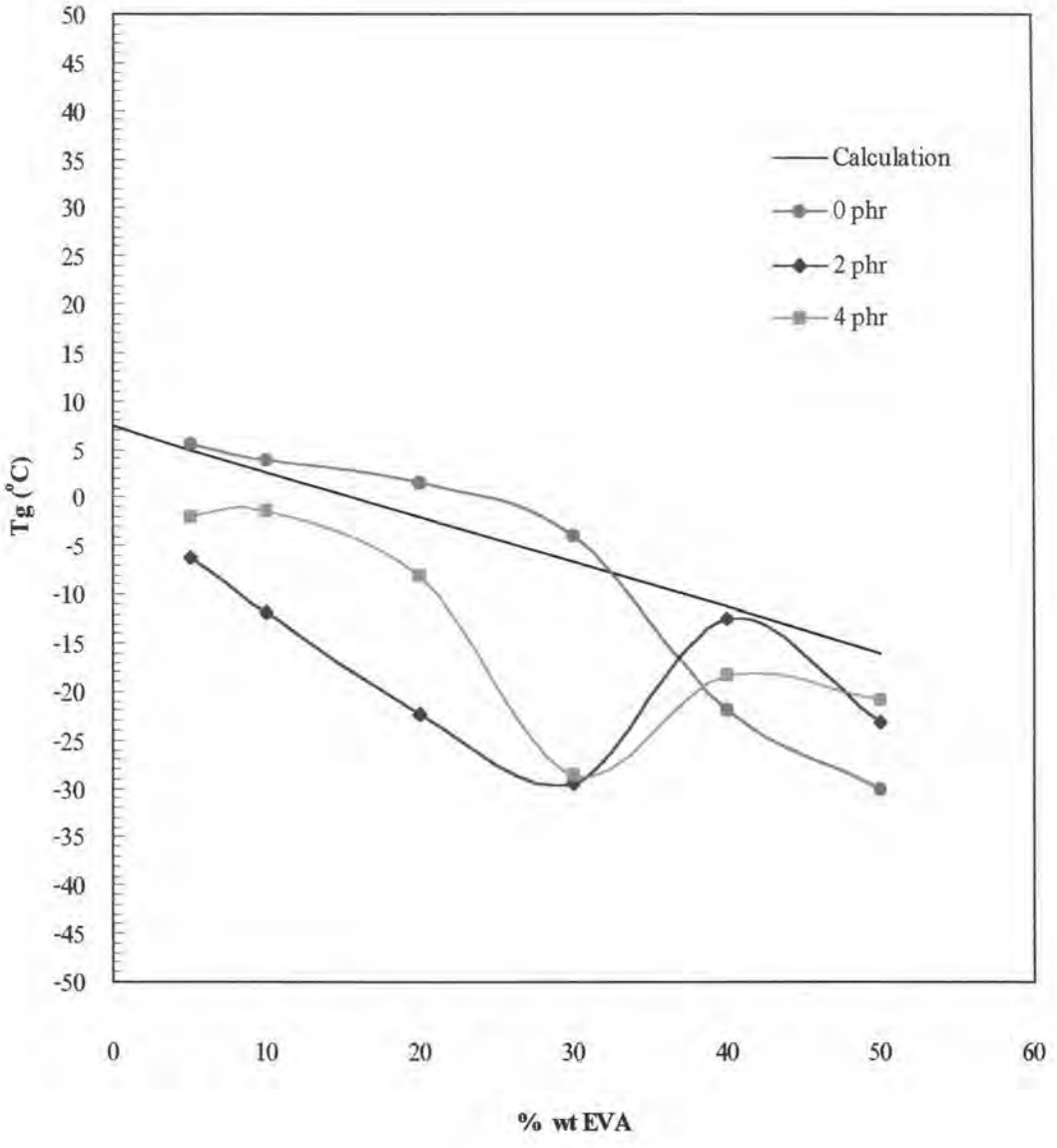

Figure 4.17 T_g of PP/EVA blend at various PP-g-MA concentrations compared with those calculated theoretically.

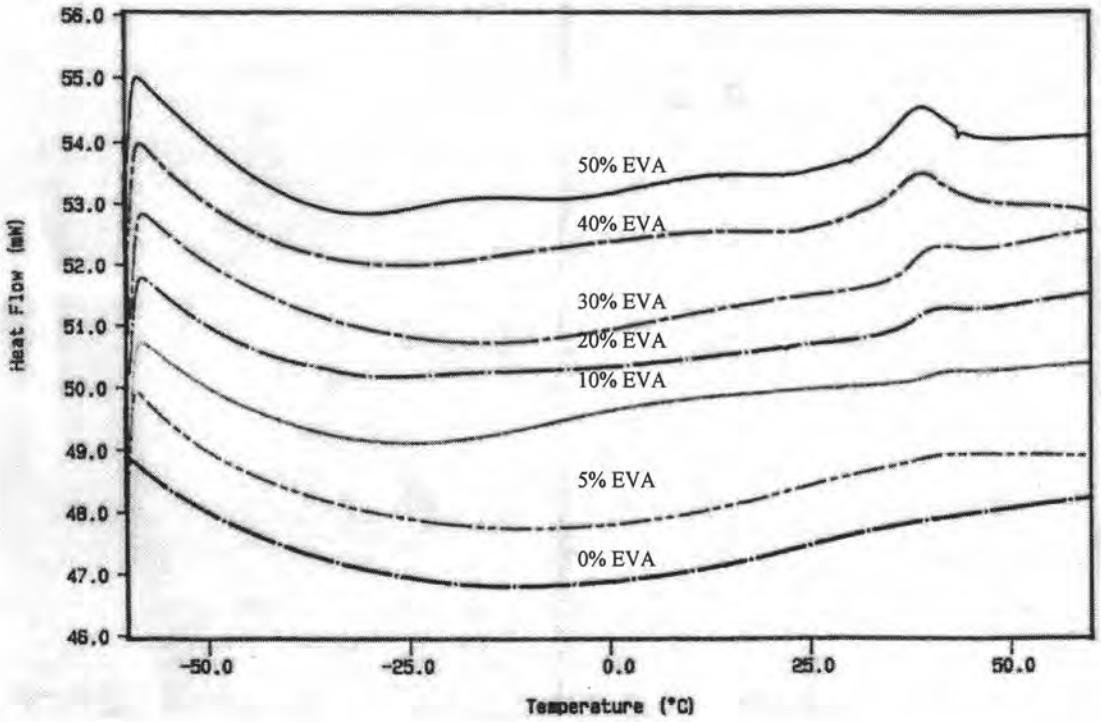

Figure 4.18 DSC thermograms exhibit the glass transition of the PP/EVA blends.

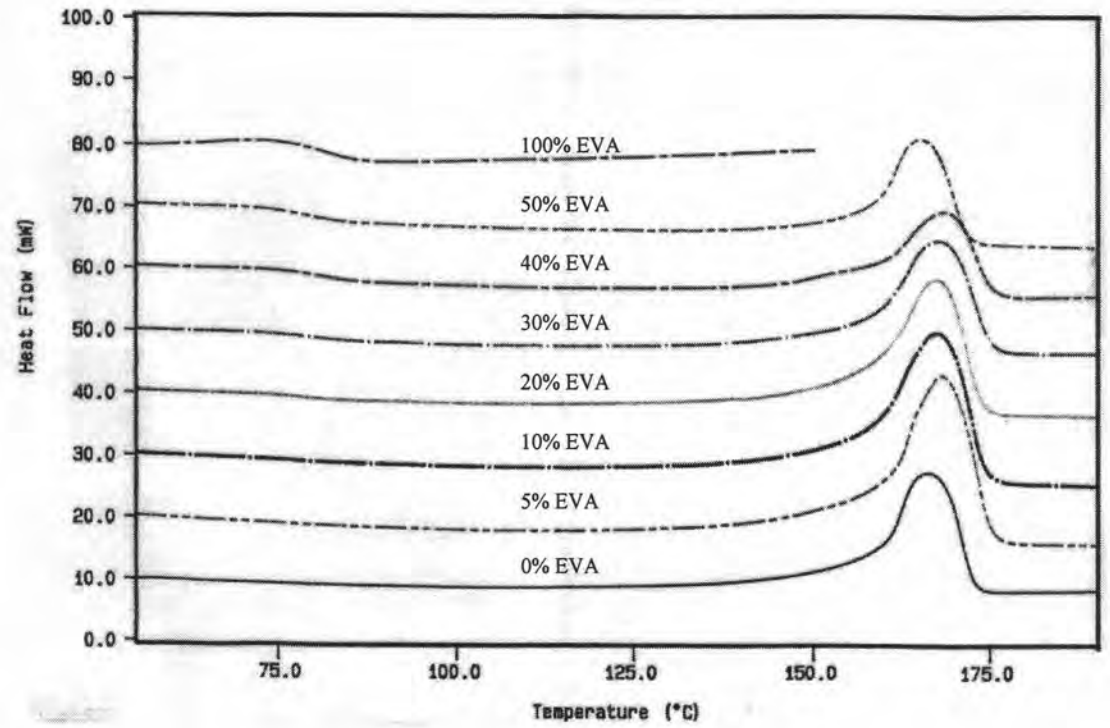

Figure 4.19 DSC thermograms exhibit the melting transition of the PP/EVA blends.

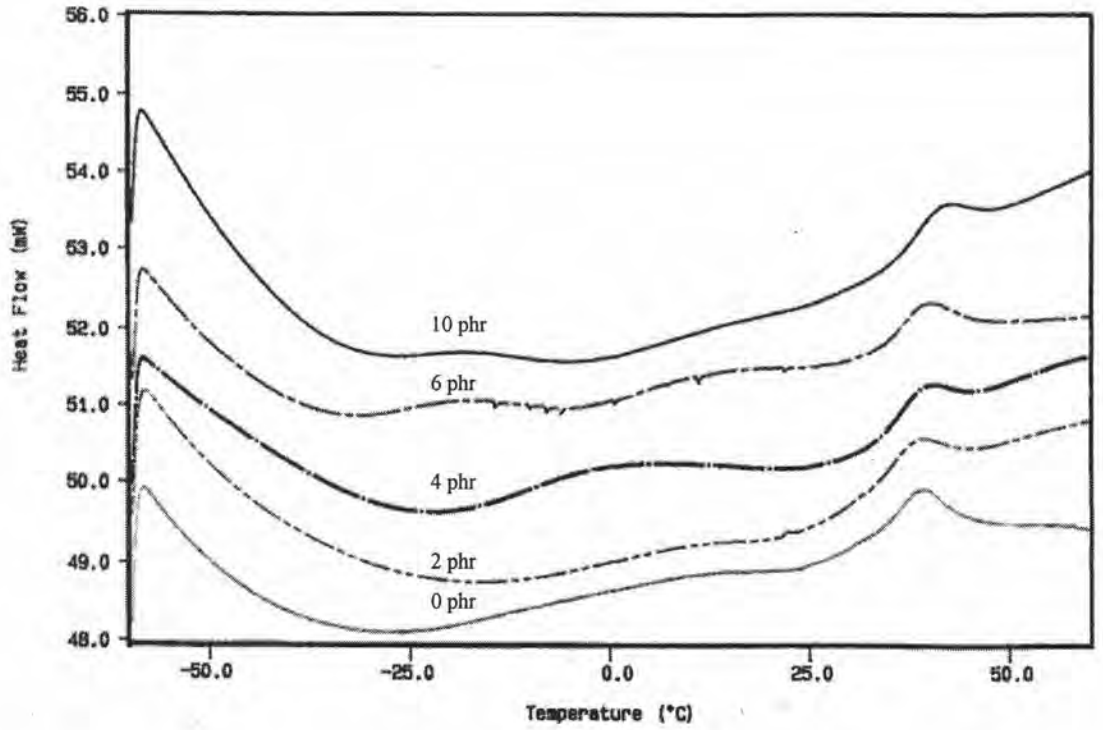

Figure 4.20 DSC thermograms exhibit the glass transition of the PP/EVA blends having 40% EVA in the blend composition. Various amount of PP-g-MA compatibilizer are labelled on the curves.

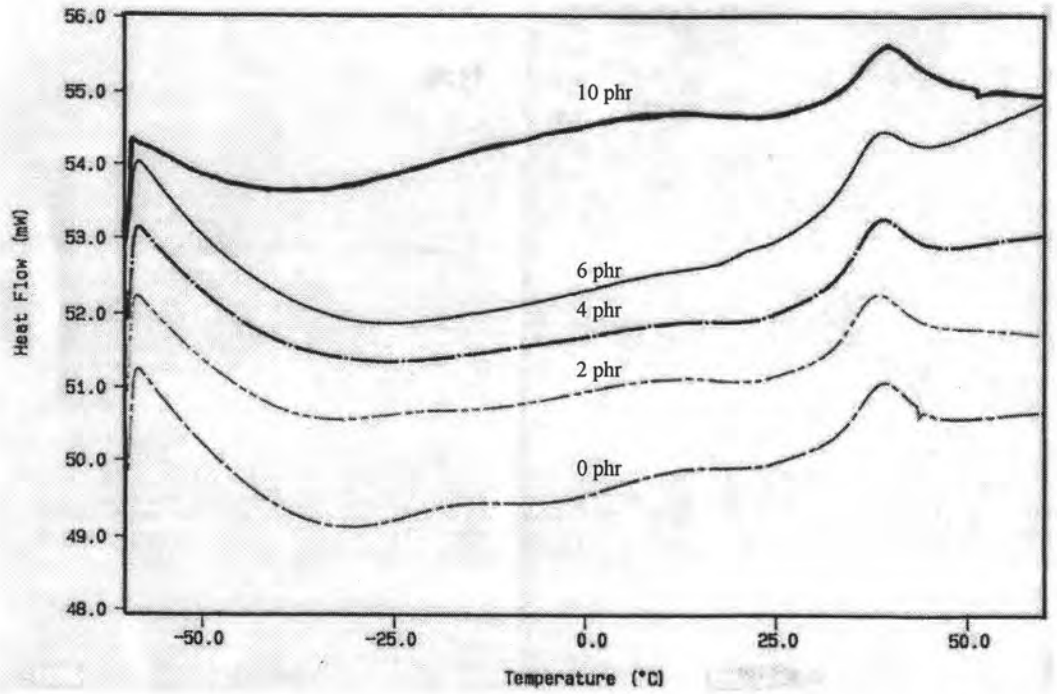

Figure 4.21 DSC thermograms exhibit the glass transition of the PP/EVA blends having 50% EVA in the blend composition. Various amount of PP-g-MA compatibilizer are labelled on the curves.

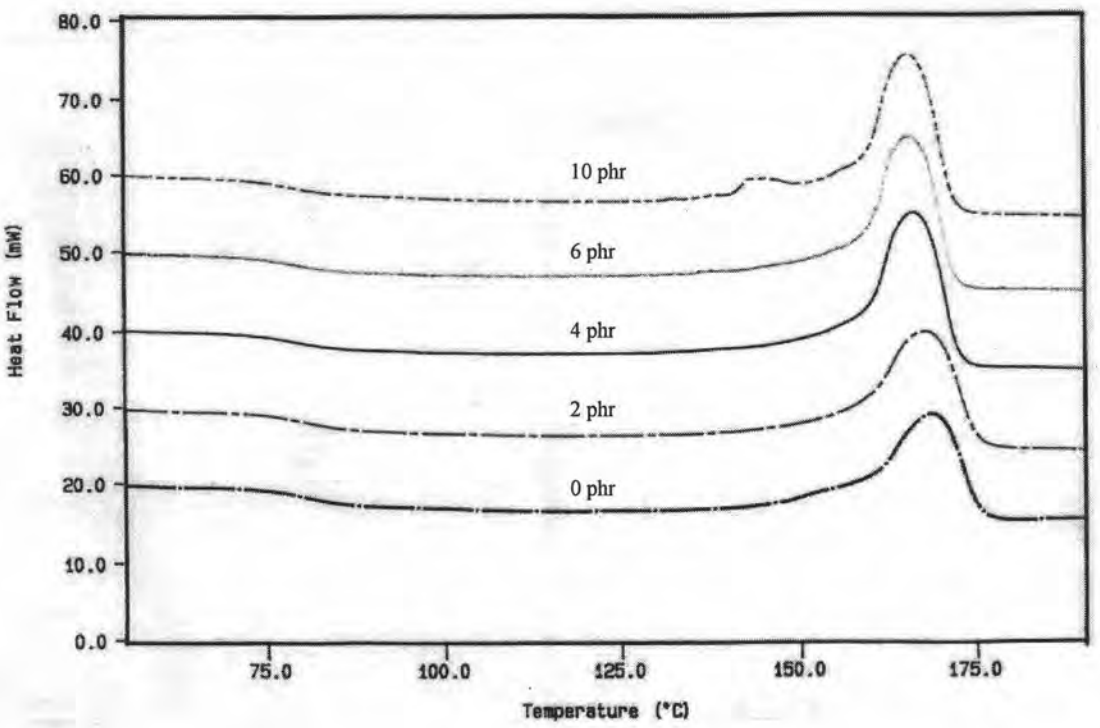

Figure 4.22 DSC thermograms exhibit the melting transition of the PP/EVA blends having 40% EVA in the blend composition. Various amount of PP-g-MA compatibilizer are labeled on the curves.

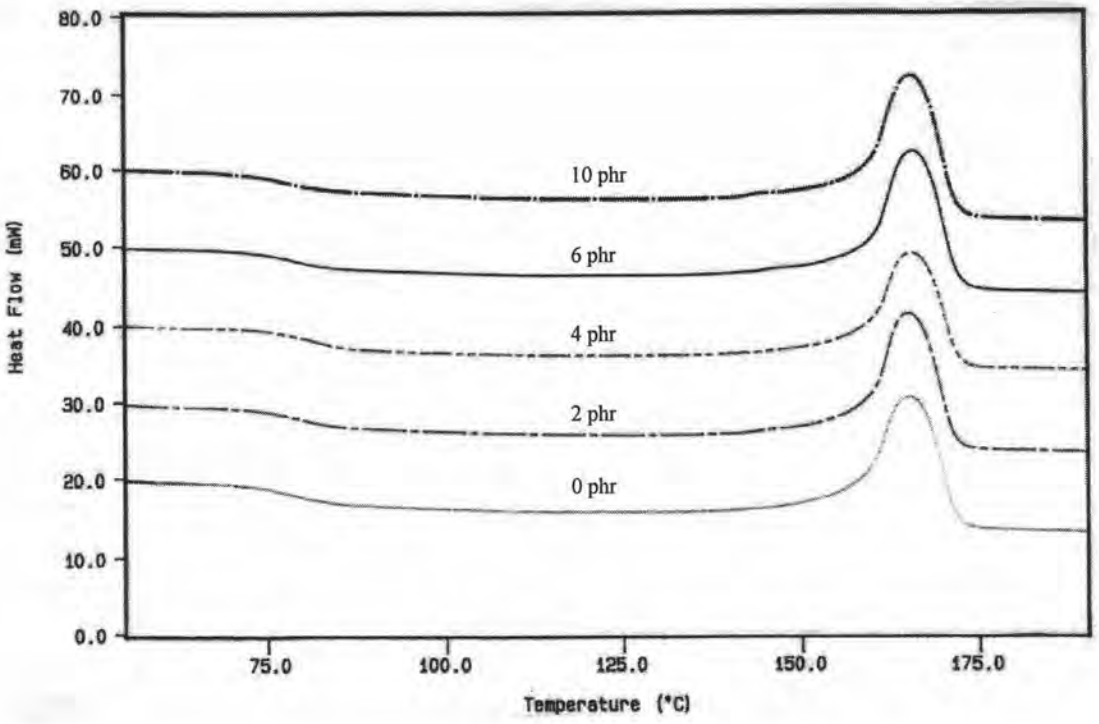

Figure 4.23 DSC thermograms exhibit the melting transition of the PP/EVA blends having 50% EVA in the blend composition . Various amount of PP-g-MA the compatibilizer are labelled on the curves.